



MULTI-AXIAL NOTCHED STRENGTH ENVELOPES FOR AEROSPACE COMPOSITE LAMINATES

A S Kaddour

*QinetiQ, Farnborough, Hampshire, GU14 0LX, UK.
e-mail: askaddour@QinetiQ.com*

Keywords: *Biaxial strength, open hole, notch, failure envelope.*

Copyright © QinetiQ Ltd 2007

Abstract

Using combined experimental and theoretical analyses, an Average Biaxial Stress Criterion (ABSC) is proposed as a method for providing a new engineering design equation for characterising the apparent magnitude of local damage around open holes in aircraft-qualified carbon/epoxy composite laminates, subjected to multi-axial loads. The experimental data were obtained from tests carried out on biaxially-loaded planar cruciforms made of T300/914 and T800/924 quasi-isotropic laminates and containing a 6mm diameter circular central hole. The theoretical analysis was based on employing a robust progressive failure model in conjunction with the classical Lekhnitskii equations for stress field around open holes. The results show that the apparent damage, represented by a characteristic distance, increases as the biaxial loading ratio deviates away from the equal biaxial points (i.e. equal tension-tension or equal compression-compression) and reaches a maximum at the equal and opposite biaxial (i.e. shear) loading point. The complete envelope of the biaxial notch strength has been established.

1. Introduction

Designers of light-weight composite structures, currently employed in aerospace and other industries, have tirelessly been seeking to establish design allowables, especially the biaxial notch strength of composites under multi-axial loads. Its importance stems from the fact that, in most applications, notches in composites are common features and/or design drivers. Notches take various

forms such as an open hole or a damaged area arising from impact by foreign objects. Bolted joints are also another clear example of why it is important to establish the multi-axial notch strength as a significant parameter in the initial, as well as, in the final sizing of a composite structure.

It is well recognised that the anisotropic nature of composites gives rise to elastic stress concentrations around open holes that are different to those encountered in isotropic materials. Depending upon lay-up and the geometry of the composites, the elastic stress concentration factors could range from around two thirds to more than twice that in metals for the same loading configuration. However, designing composites based on the elastic stress concentration alone leads to an undesirable cost ineffectiveness and hence to under-utilisation of the material, which effectively defeats one of the main reasons why composites are elected as a lightweight material in the first place.

Damage occurrence and stress relief around holes is a common phenomenon and their presence can be beneficial in reducing the magnitude of the elastic stress concentration. A complex damage pattern is usually developed around an open hole in a multi-directional laminate when the latter is subjected to remote loading cases. Matrix cracking, fibre splitting, fibre tensile fracture, fibre kinking, fibre buckling and delamination are all modes of damage that could take place around the hole, as cited in a number of publications, e.g. [1-3]. The resulting residual strength is termed as the notch strength or occasionally as the open-hole strength (normally abbreviated as OHT for uniaxial tension and OHC for uniaxial compression). The establishment of this strength, in the presence of

stress relief, is of paramount importance to designers, as it represents a common engineering property or material design allowable. Hence, a relatively large amount of research has been carried out to determine the notch strength under uniaxial loading; see for instance refs[1-3]

However, the establishment of reliable values for that strength under multi-axial load has so far received little attention, especially in terms of generating test data for a wide range of loading conditions. This is largely attributed to a lack of testing facilities capable of providing the right level of loading ratio and the instrumentation associated with it. In the absence of having reliable predictive methods for obtaining the notch strength, uni-axially loaded coupon specimens have been traditionally employed to establish material design allowables. Normally, the tests involve an expensive programme for testing many coupons with and without holes. In cases where some predictive capabilities existed, previous researchers [1-3] resorted to expressing the relationship between the *uniaxial* notched and un-notched strength via what is called the characteristic length of damage around holes. That has been applied to mainly uniaxial tension or compression loadings. Unfortunately, and in a variety of important applications, any inference of biaxial behaviour from uniaxial tests can result in unsafe design and non-conservative biaxial strength values.

To fill that gap, extensive efforts have been carried out at QinetiQ to acquire unique facilities and these efforts were made in three phases. In the first phase, a bi-axial testing machine with a capacity of 500 KN was acquired in 1993 with financial support from the UK Department of Trade and Industry (DTI) and the UK aircraft industry and the initial stage of multi-axial testing and evaluation programme was started. During Phase 1, a planar cruciform test specimen was developed that was capable of giving valid failures (i.e. failures originating from the feature under test) under the full range of bi-axial load ratios. During Phase 2, the first bi-axial test results were obtained on laminates containing open holes and filled holes (i.e. holes filled with fasteners). In Phase 3, work was carried out on thicker composites, sandwich panels, impacted panel and other filled and loaded-hole loadings where there was a strong requirement for the use of testing machines with larger capacity. A new testing machine with a capacity of 1500KN was then developed. The development of these testing

machines, specimen design and test data may be found in [4-12]. Among the tests carried out were those related to generating ultimate failure at open holes. Most of the results have been hitherto unpublished in the open literature and the present paper is concerned with providing theoretical evaluation of some of the results obtained from the three phases on multi-axially loaded laminates containing 6mm diameter holes. Further publications are planned concerning details of test data.

The combined unique biaxial testing facilities that have been recently developed and the improvement achieved in the area of validating and benchmarking the current biaxial failure theories [13], provided a strong platform for producing a reliable method for establishing the notch biaxial strength envelopes. Based on the experimental results available at key loading ratios, semi-empirical equations have been developed to describe the variation of the characteristic length around the failure envelope for both T300/914 and T800/924C quasi-isotropic laminates. The paper is aimed towards describing how the empirical equations were derived.

2. Theoretical considerations

1 Nonlinear laminate theory

Fig 1 shows a unidirectional lamina with the material coordinates. Directions 1 and 2 refer to fibre direction and transverse direction (perpendicular to fibres in the plane of the lamina), respectively. The lamina stress-strain relations are given as follows[5]:

$$\begin{Bmatrix} \sigma_1 \\ \sigma_2 \\ \tau_{12} \end{Bmatrix} = \begin{bmatrix} Q_{11} & Q_{12} & 0 \\ Q_{12} & Q_{22} & 0 \\ 0 & 0 & Q_{66} \end{bmatrix} \begin{Bmatrix} \epsilon_1 \\ \epsilon_2 \\ \gamma_{12} \end{Bmatrix} \quad (1)$$

where

$$Q_{11} = E_1 / (1 - \nu_{12}\nu_{21}),$$

$$Q_{12} = \nu_{12}E_2 / (1 - \nu_{12}\nu_{21})$$

$$Q_{22} = E_2 / (1 - \nu_{12}\nu_{21}),$$

$$Q_{66} = G_{12}$$

E_1 is the longitudinal Young's modulus,

E_2 is the transverse Young's modulus,

ν_{12} is the longitudinal Poisson's ratio,

$\nu_{21} = \nu_{12}E_2/E_1$ is the transverse Poisson's ratio,

G_{12} is the in-plane shear modulus.

The loading directions of a laminate axes are shown by the axes x and y in Fig 2. The stresses and strains of off-axis lamina in the loading directions are given by [5]:

$$\begin{Bmatrix} \sigma_x \\ \sigma_y \\ \tau_{xy} \end{Bmatrix} = \begin{bmatrix} \bar{Q}_{11} & \bar{Q}_{12} & \bar{Q}_{16} \\ \bar{Q}_{12} & \bar{Q}_{22} & \bar{Q}_{26} \\ \bar{Q}_{16} & \bar{Q}_{26} & \bar{Q}_{66} \end{bmatrix} \begin{Bmatrix} \epsilon_x \\ \epsilon_y \\ \gamma_{xy} \end{Bmatrix} \quad (2)$$

$$\begin{Bmatrix} \sigma_x \\ \sigma_y \\ \tau_{xy} \end{Bmatrix} = [T] \begin{Bmatrix} \sigma_1 \\ \sigma_2 \\ \tau_{12} \end{Bmatrix}$$

$$[\bar{Q}] = [T][Q][T]^T$$

$$[T] = \begin{bmatrix} \cos^2 \theta & \sin^2 \theta & -2 \cos \theta \sin \theta \\ \sin^2 \theta & \cos^2 \theta & 2 \cos \theta \sin \theta \\ \cos \theta \sin \theta & -\cos \theta \sin \theta & \cos^2 \theta - \sin^2 \theta \end{bmatrix},$$

$$[T]^{-1} = [T(-\theta)].$$

Using classical laminate theory, Ref[5], the forces per unit length in the i -th direction, N_i , are given by

$$N_i = \int_{-t/2}^{t/2} \sigma_i dz = \sum_{k=1}^N \left\{ \int_{z_{k-1}}^{z_k} (\sigma_i)_k dz \right\} \quad (3)$$

Where t =laminate thickness, $(\sigma_i)_k$ = i^{th} stress component in the k^{th} ply, z_{k-1} =distance from middle surface to inner surface of the k^{th} ply and z_k =distance from middle surface to outer surface of the k^{th} ply. The relationship between loads, extensional stiffness and mid-plane strains are given as[5]

$$\begin{Bmatrix} N_x \\ N_y \\ N_{xy} \end{Bmatrix} = \begin{bmatrix} A_{11} & A_{12} & A_{16} \\ A_{12} & A_{22} & A_{26} \\ A_{16} & A_{26} & A_{66} \end{bmatrix} \begin{Bmatrix} \epsilon_x^o \\ \epsilon_y^o \\ \epsilon_{xy}^o \end{Bmatrix} \quad (4)$$

The laminate extensional stiffness, A_{ij} , are given by:

$$A_{ij} = \int_{-t/2}^{t/2} (\bar{Q}_{ij})_k dz = \sum_{k=1}^N (\bar{Q}_{ij})_k (z_k - z_{k-1}) \quad (5)$$

Progressive nonlinear analysis is employed to predict the strength of the virgin (un-notched) laminate. This is based on the continuum damage model for transverse matrix cracking developed by Li et al[14]. Two main sources of nonlinearities are encountered:

- (a) The first source is caused by the lamina nonlinear shear stress strain curves.
- (b) The second source is associated with post-initial failure occurrence.

A variety of failure criteria were considered and that developed by Puck and Schürmann, see Chapters 3.7 and 5.6 in ref [13] was judged to be capable of sufficiently handling the following modes of failure

- (I) Fibre tension,
- (II) Fibre compression,
- (III) Inter-fibre failure modes. These modes describe the relationships between the transverse tension, transverse compression and shear stresses and are given as:

- (1) Mode (A) is associated with failure under combined shear and transverse tension.
- (2) Mode (B) describes failure under predominant in-plane shear stress.
- (3) Mode (C) describes the failure under predominantly transverse compression stresses.

2 Average stress criterion(ASC)

Previous studies have employed what is called the average stress criterion (ASC), introduced by Whitney and Nuismer [3], to obtain the notched strength of a laminate under uniaxial stress. The criterion is based on the assumption that failure occurs when the average stress value of σ_x over some distance a_0 , measured from the edge of the hole, reaches the un-notched uniaxial tensile strength of the material, σ_0^{un} , (see Fig 3). The criterion is expressed as [3]

$$\frac{1}{a_0} \int_R^{R+a_0} \sigma_x(y,0) dy = \sigma_0^{\text{un}} \quad (6)$$

The ratio of notched to un-notched strength is thus given by, Ref[3]

$$\frac{\sigma_N^{\text{no}}}{\sigma_0^{\text{un}}} = \frac{2(1-\xi_1)}{2-\xi_1^2-\xi_1^4+(K_T^\infty-3)[\xi_1^6-\xi_1^8]} \quad (7)$$

Where $\xi_1 = \frac{R}{R+a_0}$ and K_T^∞ is the elastic stress concentration factor, Ref[15]. This factor is related to the elastic constants of the laminate.

3 Average biaxial stress criterion (ABSC)

The Average Biaxial Stress Criterion (ABSC) is an engineering method that aims at establishing the whole biaxial notched strength envelope from a few tests carried out at selected biaxial stress ratios. The ABSC states that ultimate failure takes place when the biaxial stress, averaged over a given distance from the hole's edge, reaches the final biaxial strength of the un-notched laminate. This critical distance is dependent upon the loading ratio. The method, as presented in its current form, does not consider any mechanism of failure, on a ply level, but seeks to deal with the composite laminate as a monolithic material.

For a successful application of the method, the following prerequisite requirements should be met:

(a)- Possession of reliable failure criterion capable of predicting the ultimate failure strength of a composite laminate.

(b)- An accurate method of predicting the stress variation around a hole in an anisotropic laminate.

(c)- Reliable experimental data describing the failure of a laminate with a hole at selected stress ratios.

For a laminate, with a hole of radius R subjected to a loading as shown schematically in Fig 4, the ABSC approach is simply written as follows

$$\sigma_{bia}^{un} = \frac{1}{d_0} \int_R^{R+d_0} \sigma(r, \beta) dr \quad (8)$$

Where d_0 is the extent of damage (or characteristic distance), which is a function of the biaxial loading ratio, $\sigma(r, \beta)$ is the biaxial stress at a point (r, β) away from the centre of the hole and σ_{bia}^{un} is the ultimate (final) biaxial strength of un-notched laminate at the applied stress ratio

For the determination of strength σ_{bia}^{un} , the author proposes, based on the work reported in [13],

the use of a failure theory which is combination of the phenomenologically-based approach developed by Puck and Schürmann, see Chapters 3.7 and 5.6 in [13], and that developed by Li *et al*[14].

The determination of the stress $\sigma(r, \theta)$ can be obtained by carrying out a detailed stress analysis of a laminate with a hole, using Lekhnitskii's approach [15]. The simplified (approximate) equations suggested by Soutis and his co-workers [16,17] may also be used for many of the practical lay-ups, including the present quasi-isotropic laminate.

3. Experimental details

T300/914C and T800/924C carbon/epoxy prepreg materials; produced by Hexcel Composites, were used. The mechanical properties for the unidirectional lamina are listed in Table 1. The lay-up of the laminates reported here is quasi-isotropic and contains an equal amount of 0° , 90° , 45° and -45° plies, each ply being 0.125mm thick. Total thickness of laminates ranged from 2 to 10mm, where the 10mm specimens were supplied by Airbus UK.

The specimens were in the form of cruciform, as shown schematically in Fig 5. A central hole of 6mm was drilled in the specimens. Glass/epoxy cladding was used to prevent premature failure at the re-entrant corners of the cruciform and to arrest fractures once they have grown to the edge of the test-region.

Details of the testing programme and the experimental results can be found in [6,8,9]. Basically newly-built biaxial, hydraulically driven, testing machines with 500 and 1500KN capabilities were utilised. The machines are equipped with four perpendicular arms where any desirable combination of tension and compression loading ratios can be imposed to test the specimens to destruction. The loads were measured by the load cells mounted on each arm of the machine.

Specimens were equipped with electrical resistance strain gauges to monitor strains around the hole and Fig 6 shows a typical array of strain gauges used with the specimens. The gauges were bonded to the top and bottom surfaces of the specimens.

The stresses σ_x and σ_y were obtained from the

measured strains ϵ_x and ϵ_y using the following equation

$$\begin{aligned}\sigma_x &= \frac{E_y}{1 - \nu_{xy} \nu_{yx}} (\epsilon_y + \nu_{xy} \epsilon_x) \\ \sigma_y &= \frac{E_x}{1 - \nu_{xy} \nu_{yx}} (\epsilon_x + \nu_{yx} \epsilon_y)\end{aligned}\quad (9)$$

The elastic constants (E_x , E_y , ν_{xy} and ν_{yx}) can be obtained from classical laminate theory, Ref[5]. It should be noted here that the above equations are not valid for areas where damage has taken place. For instance, as the loading increases above a certain level, a small area surrounding the hole will be subjected to damage and this would lead to a reduction in the stiffness of the composites.

4. Results

4.1 Variation of stress and strain around holes

Measured failure strains away from the edge of the hole were taken for specimens, of different thicknesses (5 and 10mm), tested under a loading ratio of +1:-1. The results show that there is no effect of thickness on the failure strains.

The variations of stresses away from edge of the hole are shown in Figs 7 for a laminate tested under +1:-1 loading ratio. In this figure, the stresses along x and y directions are plotted for a 10mm thick laminate. It is clear that, for a distance of 20mm and above, the strains (and stresses) are unaffected by the presence of the hole.

Superimposed on the test data are theoretical curves describing the elastic behaviour of the laminate, obtained from the application of Lekhnitskii's equations. The test results are obtained from strain gauges bonded to the surfaces of the specimens. The level of measured strains at which the stresses were computed was taken to be within the linear range of the measured load-strain curves. In these figures, the predicted stresses away from the hole's edge was assumed to be identical with the measured stress away from the hole's edge. In other words, the predicted curves were forced to pass through the 'far field' measured data, as this data is unaffected by the stress concentration at the

boundary of the hole. Both the theoretical and measured data exhibited the same trend and are in a good agreement. As expected, the theoretical elastic stress concentration at the hole edge for +1:-1 loading ratio is 4. As will be shown later, the measured stress concentration, with the presence of stress relief around the hole, for this loading case, defined as the un-notched strength (457MPa) to the notched strength (260MPa), is around 1.76

4.2 Characteristic length determination

The strains measured in the tests were converted into stresses and these were used to obtain values for the characteristic distance at various loadings. Two approaches were used to obtain the variation of the characteristic length with stress ratio and these are based on linear and nonlinear regression analyses.

For the linear regression analysis, the loading ratios are divided into two zones. The first zone is that dominated by compressive fibre failure which runs from equal biaxial tension-compression point (+1:-1 loading ratio) to equal biaxial compression (-1:-1 loading ratio). The other zone is that dominated by tensile fibre failure and runs from equal biaxial tension-compression (+1:-1 loading ratio) to equal bi-axial tension (+1:+1 loading ratio).

The results from the linear regression are described by the following two equations:

(a) For compression dominated zone:

$$d_0 = C_0 + C_1 \frac{\sigma_x}{|\sigma_y|} \quad (10)$$

(b)- For the tension dominated regime ($\sigma_x > 0$):

$$d_0 = T_0 + T_1 \frac{\sigma_y}{\sigma_x} \quad (11)$$

The values of C_0 and C_1 are 3.15 and 3.10, for T300/914 material, and 3.1 and 2.9, for the T800/924C, respectively. Both equations give a value for d_0 of around 3.1 for uniaxial compression loading.

For T800/924C material, the values of T_0 and T_1 are 5.01 and -1.79, respectively. The latter equation shows that the slope of the lines is much

smaller than that observed in the compression dominated area. Those for the T300/914C are not currently available.

There are two disadvantages of the linear regression analysis (a) due to scatter in the results, the curves from the two zones did not intersect at the same point and hence this analysis does not seem to capture the precise nature of the failure points and (b) two different definitions of the biaxial ratio had to be used in order to avoid dividing a known quantity by zero. Hence, the linear regression has its own drawbacks.

The second and alternative approach is based upon using nonlinear regression analysis to generate one equation covering the whole failure envelope. This is convenient for many practical situations. The results are plotted in Fig 8 against loading ratio that is represented by the angle ψ , see Fig 9. The angle is defined as,

$$\psi = \arctan\left(\frac{\sigma_y}{\sigma_x}\right) \quad (12)$$

A second order polynomial was fitted to the results in Fig 5 and is given by

$$d_0 = M_1 + M_2 * \psi + M_3 * \psi^2 \quad (13)$$

Values for the constants M_1 , M_2 and M_3 for the T300 CFRP and T800 CFRP materials are listed in Table 2 and the range of their applicability is shown in the last column.

5. Discussion

As stated earlier, the present theoretical approach is aimed at quantifying the damage area, represented by the characteristic distance, around an open hole in biaxially loaded laminates. It should be first noted here that, for uniaxial loading, the Average Biaxial Stress Criterion (ABSC) is reduced to the classical average stress criterion (ASC) proposed by Whitney and Nuismer [3]. According to the present results, the use of a characteristic distance from uniaxial loading can lead to either overestimation or underestimation of the notch strength, depending upon the biaxial loading ratio. Hence the ABSC is a more representative criterion for describing the effects of biaxiality.

The trend presented here, where the

characteristic distance increases with biaxial stress ratio, is consistent with previous experimental and theoretical treatments. Soutis and his co-workers [16,17] developed a fracture mechanics model to predict the strength under compression-dominated loading and employed combined stable and unstable crack growth model to obtain the local damage, using point stress criterion. Their characteristic distance, based on point stress criterion, depended upon the loading condition (stress ratio). Although Soutis et al used a different approach to determine their critical crack length, their method provides a similar trend to that of the present work.

Daniel [18,19] tested quasi-isotropic carbon/epoxy laminates under two loading ratios; +1:0 and +1:+1. He observed that the characteristic distance at +1:+1 stress ratio is smaller than that at +1:0; resembling the trend shown in the present work.

Using the ABSC, the empirically determined values of d_0 obtained from the second order polynomial fit have been used to re-plot the biaxial failure envelopes, as shown in Fig. 10 for T800/924C material.

In respect of the adequacy of the test results, most of the experimental data was seen to be largely consistent and reliable. However, it was noted that the data at the -1:-1 biaxial stress ratio was lower than what one would predict and further efforts are needed to obtain more consistent values. Some difficulties were encountered in achieving a valid failure at the stress ratio -1:-1. Such difficulties had also been highlighted recently, see Chapter 7 in [13], for testing virgin quasi-isotropic laminates and recommendations were made to obtain more reliable results.

6. Conclusions

An Average Biaxial Stress Criterion (ABSC) is proposed as a method for providing a suitable design equation for characterising the apparent magnitude of local damage in aircraft qualified carbon/epoxy composite laminates, containing circular open holes and subjected to multi-axial loads.

The characteristic distance was found to depend upon the biaxial stress ratio and reaches a maximum at the equal tension-compression (i.e.

shear) loading.

The experimental results for T800/924 quasi-isotropic laminates covered most parts of the whole failure envelope.

The complete envelope of the biaxial notch strength has been established.

7. Acknowledgement

The original work reported here was carried out under Phases I, II and III of the multi-axial failure programme. Phase III was sponsored by the UK aircraft industries (Airbus UK, BAE Systems, Shorts, Hurel-Hispano and Williams GP Engineering). The author acknowledges the financial support from the MMS-5 programme, sponsored by the UK DTI.

8. References

- [1] Eriksson I and Aronsson C G, 'Strength of tensile loaded graphite/epoxy laminates containing cracks, open and filled holes', *J Compos Mater*, V24, pp 456-482, 1990.
- [2] Soutis C, Curtis P T and Fleck N A, 'Compressive failure of notched carbon fibre composites', *Proc Roy Soc Lon (A)*, V440, pp 241-256, 1993.
- [3] Whitney J M and Nuismer R J, 'Stress fracture criteria for laminated composite containing stress concentration', *J Compos Mater*, V8, pp 253-265, 1974.
- [4] Millson B J, Hopgood P J, Dadey R C and Bishop S M, 'Failure at open holes in composites under the full spectrum of biaxial loading', *DRA-SMC-CR-951076-1-0*, 1995.
- [5] Gibson R F, *Principles of Composite Material Mechanics*, McGraw-Hill, 1994.
- [6] Clarke A, Mobbs P and Coe J, 'Commissioning and performance evaluation of the 1500 kN bi-axial testing machine at MSS Farnborough', *DERA/ MSS/ MST2R/ CR990565*, Sept 1999.
- [7] Lord S J, Greenhalgh E S, Singh S and Soutis C, 'Mechanical properties of composites with stress concentrators under biaxial loading', *DERA/MSS3/ CR980710.10*, 1998.
- [8] Hopgood P, Cook J and Clarke A, 'Multi-axial testing of planar composite specimens', *ICCM12*, Paris, France, 1999.
- [9] Jones C, Clarke A and Hiley M, 'Multi-axial task C BAE open holes investigation, laboratory report', *DERA/MSS/MSTR2/CR000978*, 2000.
- [10] Kaddour A S, 'Composite Failure under Multi-axial Loading – Phase 3 Task H Report -Failure Modelling (Open Holes)', *DERA/MSS/MSTR2/CR001932*, 2000.
- [11] Kaddour A S, 'Composite failure under multi-axial loading - Phase 3 Task H Report -Failure modelling of laminates with filled holes', *DERA/ MSS/ MSTR2/ CR002292*, 2000.
- [12] Kaddour A S, 'Composite failure under multi-axial loading - Phase 3 Task H Report -Failure modelling (Pin-loaded holes)', *DERA/ MSS/ MSTR2/ CR003377*, 2000.
- [13] Hinton M J, Kaddour A S and Soden P D, '*Failure criteria for fibre reinforced polymer composites: The World-Wide Failure Exercise*', Published by Elsevier Ltd, Oxford, UK, 2004.
- [14] Li S Reid S R and Soden P D, 'A continuum damage model for transverse matrix cracking in laminated fibre reinforced composites', *Phil. Trans R Soc. Lond.*, V356, pp2379-2412, 1998.
- [15] Lekhnitskii SG, 'Theory of elasticity of an anisotropic body', Moscow, Mir Publisher; 1981. (translated from Russian).
- [16] Soutis C, Filiou C and Pateau V, 'Strength prediction of CFRP plates with a hole under biaxial compression', *AIAA Journal*, V38, No 1, pp110-114, 2000.
- [17] Filiou C and Soutis C, 'Approximate stress solution for orthotropic open-hole laminates under biaxial loading', *Adv. Compos. Letters*, V5, No 4, pp 107-111, 1996.
- [18] Daniel I M, 'The behaviour of uni-axially loaded graphite/epoxy plates with holes', In: *ICCM-2*, pp 1019-1034, 1978.
- [19] Daniel I M, 'Behaviour of graphite/epoxy plates with holes under biaxial loading', *Exper Mech*, pp 1-8, 1980.

Table 1 Mechanical properties for unidirectional T300/914 and T800/924 composites

Properties	Material	
	T300/914C	T800/924
Longitudinal modulus E_1 (GPa)	133	155.2
Transverse modulus E_2 (GPa)	9.25	8.57
Elastic in-plane shear modulus G_{12} (GPa)	4.85	7.4
Major Poisson's ratio ν_{12}	0.3	0.36
Longitudinal tensile strength MPa	1650	1982
Transverse tensile strength MPa	34	48.7
Longitudinal compressive strength MPa	1450	1550
Transverse compressive strength MPa	200	250
Shear strength MPa	80	113

Table 1 Results of the second order regression analysis described in Equation (5)

Material	Values of the constants			Remarks
	M_1	M_2	M_3	
T800/924C	5.24	-2.42E-2	-4.626E-4	Valid for $45^\circ > \psi > -135^\circ$
T300/914C	4.428	-4.238E-2	-5.610E-4	Valid for $-135^\circ < \psi < -45^\circ$

MULTI-AXIAL NOTCHED STRENGTH ENVELOPES FOR AEROSPACE COMPOSITE LAMINATES

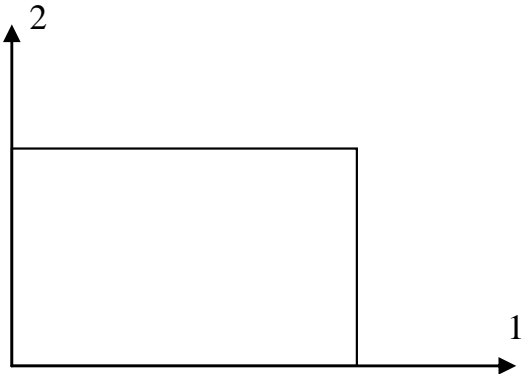


Fig 1 A unidirectional lamina in material co-ordinate system

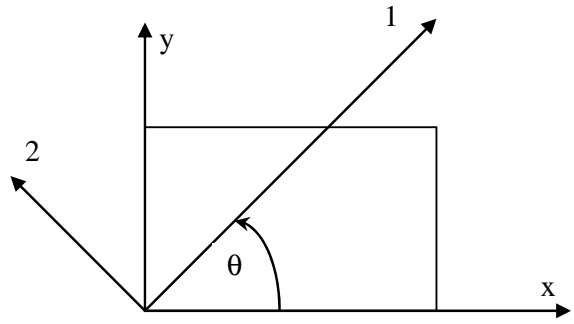


Fig 2 Schematic of off-axis lamina with coordinates system in the loading directions

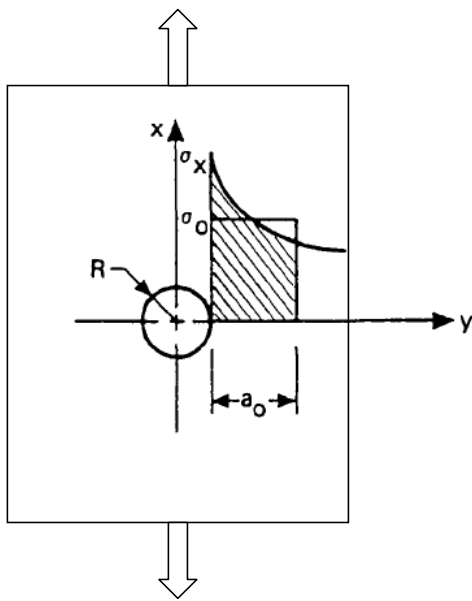


Fig 3 A laminate containing an open hole subjected to uniaxial tension and an illustration of average stress criterion.

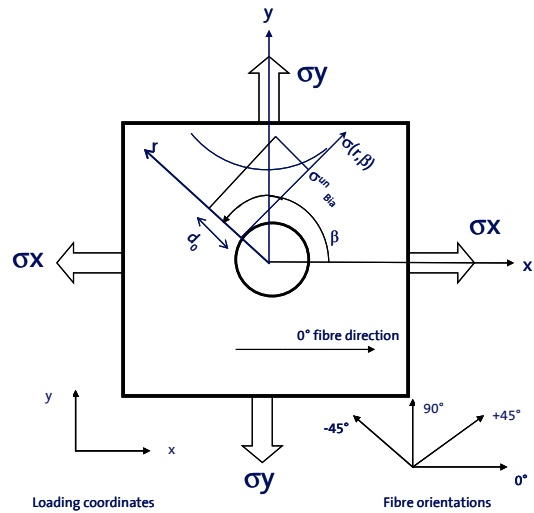


Fig 4 A schematic showing material and loading coordinates of a laminate, containing an open hole, under biaxial loads

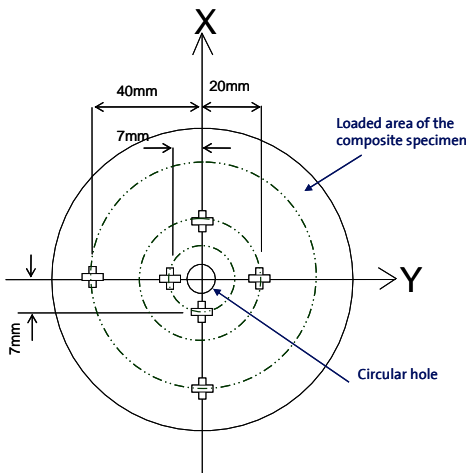


Fig 6 Schematic illustrating locations of strain gauges around the central hole

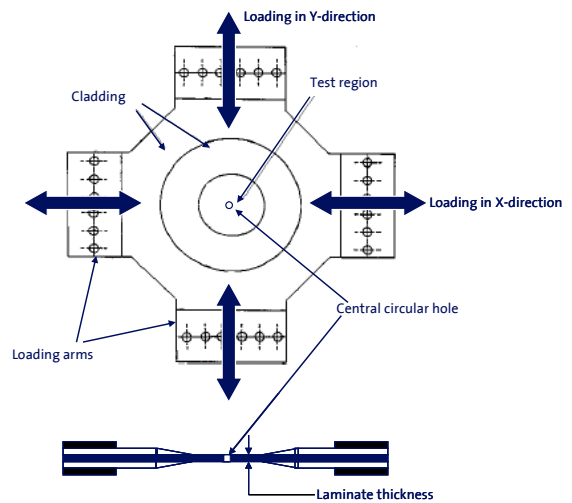


Fig 5 A schematic of the biaxial cruciform specimen showing the loading area and the loading configuration.

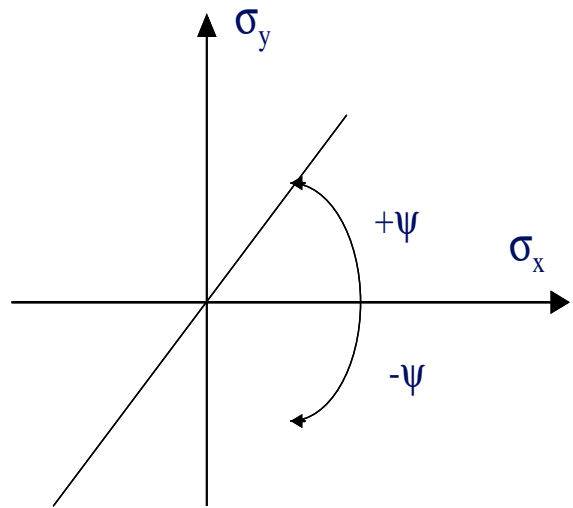
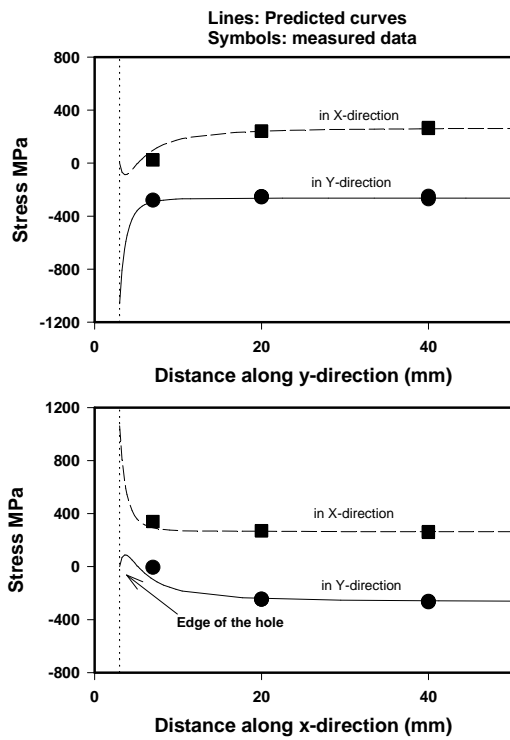


Fig 9 Schematic of how the angle ψ , representing the biaxial stress, is measured

Fig. 7 Variation of stresses away from the centre of specimen tested under +1:-1 loading ratio

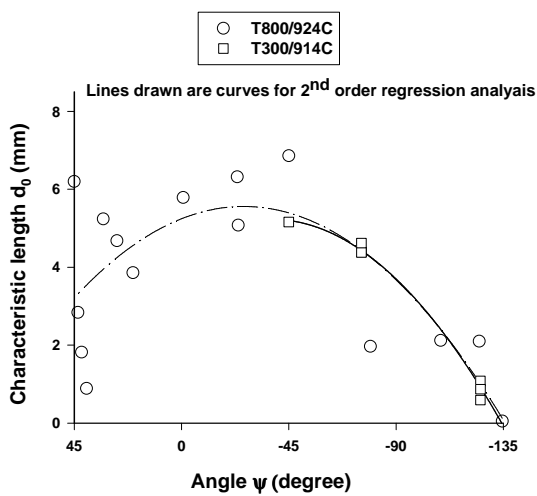


Fig 8 Variation of the characteristic length d_0 with applied stress ratio, represented by an angle ψ , for two materials.

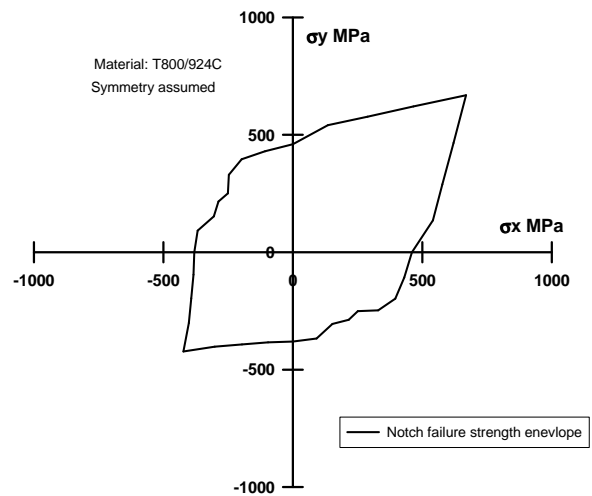


Fig 10 Biaxial notched failure envelope for T800/924 Carbon/epoxy material.